



Synthesis, Characterization and Antimycobacterial Activity of Phenanthrenequinone Thiosemicarbazones and their Ruthenium and Zinc Complexes

ASHOK K. SINGH^{1,*}, SHAILENDRA K. SINGH¹, KAVITA DHARIYAL¹, RAM KUMAR², AMARENDRA KUMAR¹ and SUDHEER K. SINGH²

¹Department of Chemistry, University of Lucknow, Lucknow-226007, India

²Microbiology Division, CSIR-Central Drug Research Institute, Sitapur Road, Lucknow-226031, India

*Corresponding author: E-mail: singhaks3@rediffmail.com

Received: 18 January 2021;

Accepted: 11 February 2021;

Published online: 16 April 2021;

AJC-20314

The substituted phenanthrenequinone thiosemicarbazones (HL1, HL2 and HL3), and their metal complexes (M = Ru(II) or Zn(II); SM1, SM2, SM3 and SM4) were synthesized and characterized by FT-IR, ¹H & ¹³C NMR and ESI-MS. The spectral data IR, ¹H & ¹³C NMR and ESI-MS indicates two tridentate ligands coordinating in the form of an octahedral geometry. The gas phase geometry of all the zinc(II) and ruthenium(II) complexes was carried by using density functional theory (DFT). The antimycobacterial susceptibility testing at 100 μM of the complexes using resazurin microtiter plate assay resulted in growth inhibition. Complexes SM2, SM3 and SM4 showed good antimycobacterial activity at 100 μM concentration by using rifampicin as inhibition control.

Keywords: Phenanthrenequinone, Thiosemicarbazones, Ruthenium complexes, Zinc complexes, Antimycobacterial, Rifampicin.

INTRODUCTION

Tuberculosis (TB) caused by *Mycobacterium tuberculosis* (*Mtb*) is one of the major causes of deaths due to transferrable diseases in developing countries. In year 2019, nearly 1.4 million people (eliminating 0.3 million deaths affected by HIV-TB complex) deceased due to tuberculosis while 10 million (5.6 million men, 3.2 million women, 1.2 million children) new cases were also reported. The microorganism has developed incredible mechanisms to avoid being cleared by host immune response and can remain dormant for long periods of time [1]. This makes its treatment very difficult. The improvement of drug resistance has further complicated the current therapeutic approaches, making the need of new drugs to treat tuberculosis and crucial priority in the drug development [2]. *Mycobacterium tuberculosis* H37Ra (*Mtb*-Ra) is a virulent strain of *Mtb*, which can be appropriately employed to test potency of new inhibitors [3]. The 96-well plate based resazurin microtiter plate assay (REMA), for antimycobacterial drug susceptibility testing, is a cost effective and wild method, to test effectiveness of new compounds against *Mtb*. Rifampin and isoniazid are well known drugs used in treatment of tuberculosis [4]. Although very effective these drugs cause many side effects such as diarrhoea,

loss of appetite, blurred vision and many allergic reactions [5]. In order to minimize these side effects, new complexes with other transition metals are being synthesized [6]. Among them, Zn(II) and Ru(II) metal complexes offer facile synthesis and possess medicinal characteristics. Presently, Zn(II) and Ru(II) complexes are the objective of great attention in the field of medicinal chemistry with low systematic toxicity [7,8].

From long time and till now, the research on Schiff base ligands is of sharp consideration since they are known as the most special ligands in the coordination chemistry due to their easy method of synthesis by condensation reaction between carbonyl and amines. Quinonoid compounds are the second biggest class of anticancer agents. The cytotoxicity of these compounds is explained based on numerous mechanisms including intercalation, hindrance of DNA and RNA, breaking of DNA strands [9,10]. 9,10-Phenanthrenequinone, are additionally known to form many type of transition metal complexes but these metal complexes are relatively less known [11]. The metal chelation properties are improved when one of the carbonyl oxygen is reacting with thiosemicarbazide to form phenanthrenequinone thiosemicarbazone [11-14]. Although, several promising results had been reported, the Zn(II) and Ru(II) compounds bearing thiosemicarbazide ligands, which offered

in vivo anticancer and *in vitro* antibacterial activity have been carried out [15-17]. In this work, the synthesis and characterization of some ruthenium(II) and zinc(II) complexes with 9,10-phenanthrenequinone thiosemicarbazones and its antimycobacterial activity are reported.

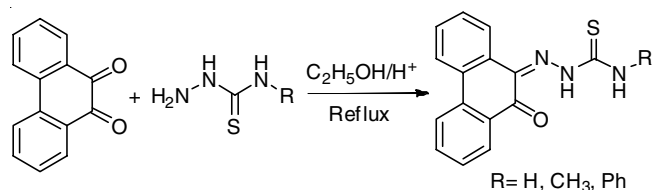
EXPERIMENTAL

All chemicals were purchased from several reputed commercial suppliers *viz.* Sigma-Aldrich, Spectrochem, Alfa-Aesar and Merck, and used without purification. Solvents were purified and dried accordingly by reported procedure. FT-IR and ¹H NMR spectra were recorded on Agilent Cary 630 FT-IR and Bruker-AVLL-300 MHz (DMSO-*d*₆), spectrometer using TMS as an internal reference. Elemental analysis was performed on Euro-Vector analyzer. ESI-MS spectrometry was performed on WATERS UPLC-TQD MASS spectrometer. Electronic absorption spectra were recorded on Labtronic-2900-UV-Vis spectrophotometer. All the biological activities were carried out from Microbiology division, CSIR-CDRI, Lucknow, India.

Antimycobacterial drug susceptibility testing: The antimycobacterial drug susceptibility test was performed using resazurin microtiter plate assay with acetate as a carbon source [17]. The *Mycobacterium tuberculosis* H37R a log phase culture grown in Sauton's medium with glycerol as a carbon source was pelleted and washed twice with Sauton's medium with acetate as a carbon source, subsequently the pellet was diluted with the same medium to give an OD₆₀₀ of 0.10 and 100 μL and taken in microtiter plate. The Sauton's medium (100 μL) with acetate as a carbon source was used for inhibition studies. The compound concentration was initially adjusted to 100 μM. The sterility control, growth control and solvent controls were also included and all the experiments were performed in triplicates. The plates were sealed properly and incubated for 5 days at 37 °C. After completion of incubation 25 μL of resazurin (0.03 % w/v) was added to suspension and mixed and fluorescence was recorded after 5 h at (535/595 excitation/emission) using a fluorescence plate reader (BMG Omega plate reader). The MIC was estimated by serially diluting compounds to a final concentration of 100, 50, 25, 12.5, 6.25 and 3.125 μM. The MIC₉₀ was calculated as the concentration of compound, which caused greater than 90% reduction in fluorescence of culture.

Synthesis of phenanthrenequinone thiosemicarbazone:

The substituted thiosemicarbazide (1 mmol, 133 mg) and phenanthrenequinone (1 mmol, 300 mg) in 20 mL ethanol were refluxed on oil bath for 6 h. It was kept for overnight when a brown colour crystalline product of Schiff base separated out, which was filtered, purified with diethyl ether and cold ethanol and dried in vacuum (**Scheme-I**).



Scheme-I: Synthetic route of phenanthrenequinone thiosemicarbazone ligands

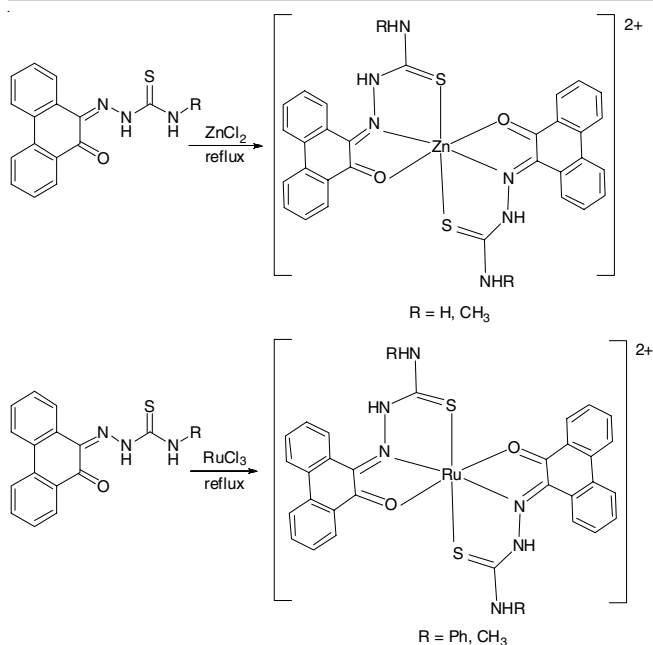
(Z)-2-(10-Oxophenanthren-9(10H)-ylidene)hydrazine carboxamide (HL1): Colour: brown, yield: 87% (300 mg), m.p.: 180 °C. IR (KBr, cm⁻¹, ν_{max}): 3392, 3265 (NH₂), 3153 (NH), 1678 (CO), 1593 (CN), 835 (CS); ¹H NMR (300 MHz, DMSO-*d*₆), δ ppm: 11.02 (N-H, 1H, s), 8.31-8.17 (NH₂, 2H, s), 7.88 (Ar-H, 5H, m), 7.48-7.44 (Ar-H, 1H, s), 7.26 (Ar-H, 1H, s) 7.06-7.02 (Ar-H, 1H, d); ¹³C NMR (75 MHz, DMSO-*d*₆), δ ppm: 183.80, 178.80, 168.80, 160.80, 156.05, 148.19, 144.19, 138.74, 134.78, 125.78, 122.75, 121.75, 120.71, 116.41, 106.45; Elemental analysis of C₁₅H₁₁N₃OS calcd. (found) (%): C, 64.04 (64.05); H, 3.94 (3.96); N, 14.94 (14.96); O, 5.69 (5.71); S, 11.40 (11.41); ESI-MS: [M + 1]⁺ m/z: 283 (obs.); calcd. (282). UV-vis.: λ_{max} in nm (DMSO, 10⁻³ M), 190 (π-π* transitions), 283 (π-π* transitions), 294 (π-π* transitions), 370 (n-π* transition).

(Z)-N-Methyl-2-(10-oxophenanthren-9(10H)-ylidene)hydrazine carboxamide (HL2): Colour: orange, yield: 87% (295 mg), m.p.: 182 °C. IR (KBr, cm⁻¹, ν_{max}): 3378, (NH₂), 3019 (NH), 1677 (CO), 1597 (CN), 926 (CS), ¹H NMR (300 MHz, DMSO-*d*₆), δ ppm: 11.17 (N-H, 1H, s), 8.31 (N-H, 1H, s), 7.88 (Ar-H, 1H, s), 7.64-7.44 (Ar-H, 5H, m), 7.26 (Ar-H, 1H, s), 7.06-7.02 (Ar-H, 1H, d), 3.18 (N-CH₃, 3H, s); ¹³C NMR (75 MHz, DMSO-*d*₆), δ ppm: 180.83, 14.82, 168.19, 161.08, 145.12, 144.19, 138.87, 134.74, 127.74, 122.79, 121.78, 120.15, 106.45; Elemental analysis of C₁₆H₁₃N₃OS calcd. (found) (%): C, 65.06 (65.08); H, 4.44 (4.45); N, 14.23 (14.22); O, 5.42 (5.44); S, 10.86 (10.87); ESI-MS m/z: 296 (obs.), calcd. (295). UV-vis.: λ_{max} in nm (DMSO, 10⁻³ M), 194 (π-π* transitions), 284 (π-π* transitions), 290 (π-π* transitions), 374 (n-π* transitions).

(Z)-2-(10-Oxophenanthren-9(10H)-ylidene)-N-phenylhydrazine carboxamide (HL3): Colour: dark brown, yield: 82% (284 mg), m.p.: 168 °C. IR (KBr, cm⁻¹, ν_{max}): 3364, (NH₂) 1672 (CO), 1593 (CN), 1115 (CS), ¹H NMR (300 MHz, DMSO-*d*₆), δ ppm: 11.02 (N-H, 1H, s), 8.97-8.74 (N-H, 1H, s), 8.41 (Ar-H, 4H, s), 8.31-7.41 (Ar-H, 7H, m), 7.26 (Ar-H, 1H, d), 7.06-7.02 (Ar-H, 1H, d). ¹³C NMR (75 MHz, DMSO-*d*₆), δ ppm: 183.01, 173.01, 148.88, 148.25, 147.37, 144.15, 141.92, 136.54, 133.73, 128.80, 128.42, 127.97, 125.27, 124.81, 119.34, 118.33, 116.41, 115.92, 114.43, 114.39, 113.15; Elemental analysis of C₂₁H₁₅N₃OS calcd. (found) (%): C, 70.57 (70.59); H, 4.23 (4.21); N, 11.76 (11.74); O, 4.48 (4.49); S, 8.97 (8.98); ESI-MS m/z: 357 (obs.), calcd. (358); UV-vis.: λ_{max} in nm (DMSO, 10⁻³ M), 188 (π-π* transitions), 280 (π-π* transitions), 298 (π-π* transitions), 376 (n-π* transitions).

Synthesis of metal complexes: Metal complexes of zinc(II) and ruthenium(II) (SM1, SM2, SM3, SM4) were synthesized by refluxing ethanol solution of metal salt (ZnCl₂, 1 mmol; 50 mg) with ethanol solution of ligands (HL1/HL2), (2 mmol; 238 mg / 242 mg) and (RuCl₃, 1 mmol; 60 mg), with (HL3, HL2), (2 mmol; 170 mg/192 mg), respectively for 7 h. After cooling at room temperature, respective solution was dried in vacuum. The residue was isolated and washed with ethanol, diethyl ether and dried to obtain the desired metal complexes (**Scheme-II**).

[Zn(HL1)]Cl₂ (SM1): Colour: orange, yield: 62% (156 mg), m.p.: > 320 °C, IR (KBr, cm⁻¹, ν_{max}): 3386 (NH₂), 3020 (NH), 1515 (CO), 1426 (CN), ¹H NMR (300 MHz, DMSO-*d*₆), δ ppm: 11.42 (N-H, 2H, d), 8.31-8.20 (NH₂, 1H, d), 8.14-



Scheme-II: Synthetic route of metal(II) metal complexes of phenanthrenequinone thiosemicarbazone

8.02 (NH₂, 1H, d), 7.86-7.76 (Ar-H, 7H, m), 7.42-7.26 (Ar-H, 1H, d), 7.06-6.92 (Ar-H, 10H, m). ¹³C NMR (75 MHz, DMSO-*d*₆), δ ppm: 180.00, 176.88, 168.40, 160.80, 156.75, 148.19, 144.19, 138.47, 134.87, 125.78, 122.44, 121.57, 120.41, 116.71, 106.54; Elemental analysis of C₄₂H₂₂N₆S₂Zn₂ calcd. (found) (%): C, 51.96 (51.97); H, 3.20 (3.21); N, 12.12 (12.15); O, 4.61 (4.61); Zn, 18.86 (18.87); S, 9.25 (9.26); ESI-MS: 625 (Obs.), 625 (calcd.). UV-vis.: λ_{\max} in nm (DMSO, 10⁻³ M); 192 (π - π^* transitions).

[Zn(HL2)]Cl₂ (SM2): Colour: dark brown, yield: 69% (174 mg), m.p.: > 360 °C, IR (KBr, cm⁻¹, ν_{\max}): IR (KBr, cm⁻¹, ν_{\max}): 3391 (NH₂), 3020 (NH), 1643 (CO), 1527 (CN). ¹H NMR (300 MHz, DMSO-*d*₆), δ ppm: 11.67 (N-H, 2H, d), 7.97-7.80 (NH, 2H, s), 7.69-6.34 (Ar-H, 16, m), 2.97 (N-CH₃, 6H, s); ¹³C NMR (75 MHz, DMSO-*d*₆), δ ppm: 180.83, 174.82, 168.19, 161.08, 145.12, 144.19, 138.87, 134.74, 127.74, 121.78, 120.15, 105.46, 32.56; Elemental analysis of C₃₂H₂₆N₆S₂Zn₂ calcd. (found) (%): C, 53.27 (53.28); H, 3.63 (3.64); N, 11.65 (11.66); O, 4.44 (4.45); Zn, 18.12 (18.13); S, 6.99 (6.97); ESI-MS *m/z*: 655 (Obs.), 655 (calcd.). UV-vis.: λ_{\max} in nm (DMSO, 10⁻³ M), 200 (π - π^* transitions).

[(Ru(HL3)]Cl₂ (SM3): Colour: black, yield: 63% (163 mg), m.p.: > 388 °C, (KBr, cm⁻¹, ν_{\max}): 3398 (NH₂), 3020 (NH), 1677 (CO), 1448 (CN), ¹H NMR (300 MHz, DMSO-*d*₆), δ ppm: 11.42 (N-H, 2H, d), 8.31-7.86 (NH, 2H, s), 7.86-7.76 (Ar-H, 10H, m), 7.42-7.26 (Ar-H, 9H, m), 7.06-6.76 (Ar-H, 7H, m), ¹³C NMR (75 MHz, DMSO-*d*₆), δ ppm: 180.01, 172.88, 148.01, 147.37, 144.14, 141.92, 136.55, 133.73, 128.80, 128.43, 125.97, 125.27, 124.81, 119.32, 118.33, 116.41, 114.39, 113.15; Elemental analysis of C₄₂H₃₀N₆S₂Ru₂ calcd. (found) (%): C, 55.01 (55.03); H, 3.30 (3.32); N, 9.16 (9.17); O, 3.49 (3.48); Ru, 22.04 (22.03); S, 6.99 (6.98); ESI-MS *m/z*: 815 (Obs.), 815 (calcd.). UV-vis.: λ_{\max} in nm (DMSO, 10⁻³ M), 192 (π - π^* transitions), 500 (CT Transition).

[Ru(HL2)]Cl₂ (SM4): Colour: black, yield: 72% (167 mg), m. p.: > 378 °C, IR (KBr, cm⁻¹, ν_{\max}): 3391 (NH₂), 3020 (NH), 1676 (CO), 1524 (CN), ¹H NMR (300 MHz, DMSO-*d*₆), δ ppm: 11.11 (N-H, 2H, d), 8.36 (N-H, 2H, s), 7.87-7.76 (Ar-H, 8H, m), 7.66-7.42 (Ar-H, 5H, m), 7.27-7.02 (Ar-H, 3H, m), 3.18 (N-CH₃, 6H, s). ¹³C NMR (75 MHz, DMSO-*d*₆), δ ppm: 180.82, 177.83, 168.81, 161.08, 147.12, 138.78, 134.74, 124.77, 122.74, 121.79, 120.51, 106.45, 32.56; Elemental analysis of C₄₂H₂₆N₆S₂Ru₂ calcd. (found) (%): C, 48.48 (48.47); H, 3.31 (3.32); N, 10.60 (10.62); O, 4.04 (4.05); Ru, 25.50 (25.51); S, 8.09 (8.07); ESI-MS *m/z*: 692 (Obs.), 691 (calcd.). UV-vis.: λ_{\max} in nm (DMSO, 10⁻³ M), 210 (π - π^* transitions), 520 (CT Transition).

RESULTS AND DISCUSSION

FTIR studies: The IR spectral data of the ligands and its metal(II) complexes indicated the formation of the complexes. The derivatives of the phenanthrenequinone with thiosemicarbazide bands observed at 3265 and 3392 cm⁻¹ in the spectrum of ligands, which are due to the asymmetric and symmetric stretches of the amino group. The presence of band at 1593 cm⁻¹ due to ν (C=N) confirms the imine group present in the ligands. The ligand phenanthrenequinone thiosemicarbazone appears as the thionic tautomer due to presence of ν (N-H) stretch at 3153 cm⁻¹ [14]. After complexation, phenanthrenequinone thiosemicarbazone ligands acts as a tridentate moiety forming two five-membered chelate rings around the central metal through a donor atom including the quinone carbonyl oxygen, imine nitrogen and the thiolate sulfur corresponding shifts in IR frequencies. For instance, the peaks of ν (C=N) and ν (C=O) vibrations appeared at 1593 and 1631 cm⁻¹, respectively separately in the spectra of the parent ligand are shifted to lower wave numbers while the groups at 835 and 1174 cm⁻¹ attributed to the ν (C=S) stretch, which disappear on coordination. Additionally, the bands between 550-450 cm⁻¹ represents M-O bonds [18-20].

NMR studies: The ¹H NMR range of ligands (HL1, HL2 and HL3) shows a singlet in the range δ 11.17-11.02 ppm due to NH group. In the spectra of metal complexes (SM1, SM2, SM3 and SM4) indicates doublet of N-H proton in the range δ 11.67-11.11 ppm possess 1:2 stoichiometry of metal to ligands composition. The phenanthrenequinone ring protons appeared in the range of δ 7.88-7.02 ppm, which showed slight shifting after metal ion coordination. There are two singlets of NH₂ groups at δ 8.36 and 8.17 ppm and the separation between these two peaks is downward shifting to δ 0.1-0.4 ppm in the spectra of SM1 metal complex, indicates lowering of the bond order due to thiolato complexation [21]. Although, NH₂ protons are not coordinated to the metal complexes, but signals become shielded because of electronic effect. ¹³C NMR of ligands shows carbonyl peaks around 183 ppm which becomes 180 ppm on metal coordination indicate carbonyl takes part in chelation during formation of metal complex, also the ¹³C NMR value of thiocarbonyl and imine shift to lower.

Mass studies: The binding of Ru(II) and Zn(II) metal ions with substituted phenanthrenequinone thiosemicarbazone was investigated by ESI-MS spectroscopy. In the mass spectrum,

the peak observed at m/z 625 arises for $[\text{Zn}(\text{HL1})]\text{Cl}_2$, m/z 655 for $[\text{Zn}(\text{HL2})]\text{Cl}_2$, m/z 815 for $[\text{Ru}(\text{HL3})]\text{Cl}_2$ and m/z 692 for $[\text{Ru}(\text{HL2})]\text{Cl}_2$. All the complexes shows $[\text{M}]^+$ molecular ion peak except $[\text{Ru}(\text{HL3})]\text{Cl}_2$, which shows $[\text{M}+1]^+$ molecular ion peak. All the above patterns of ESI-MS spectroscopy are in accordance with the other spectral data.

UV-Vis studies: The electronic spectral analysis of phenanthrenequinone thiosemicarbazones in DMSO (10^{-3}M) solvents shows intense bands in the range 294 and 370 nm for imine and thioamide $n\text{-}\pi^*$ transition, respectively [22]. These bands shift to higher wavelength upon metal coordination. In the spectra of all ruthenium(II) complexes band observed at 420-525 nm, which is characteristic of Ru(II) ion as reported earlier [23]. All the metal-complexes are binuclear with the band in the region from 200 to 525 nm. However, Zn(II) complexes do not shows any bands because of its d^{10} electronic arrangements [24].

Computational studies

Geometry optimization: The density functional theory (DFT) calculations have been performed for metal complexes (SM1-SM4) in the gas phase by using of B3LYP and LANL2DZ basis set. The selected interatomic distances and bond angles for all metal complexes are shown in Table-1. The calculated bond distances between Ru-N and Ru-O phenanthrenequinone thiosemicarbazone are 2.286-2.293 Å and 2.147-2.152 Å, respectively. Moreover, the Zn-N and Zn-O bond distances of phenanthrenequinone thiosemicarbazones ligand are 2.032-2.030 Å and 2.124-2.131 Å, respectively. These results showed that the computed structural parameters are reliable with the single X-ray data of associated structures [25]. The optimized geometry of the synthesized metal(II) complexes are shown in Fig. 1.

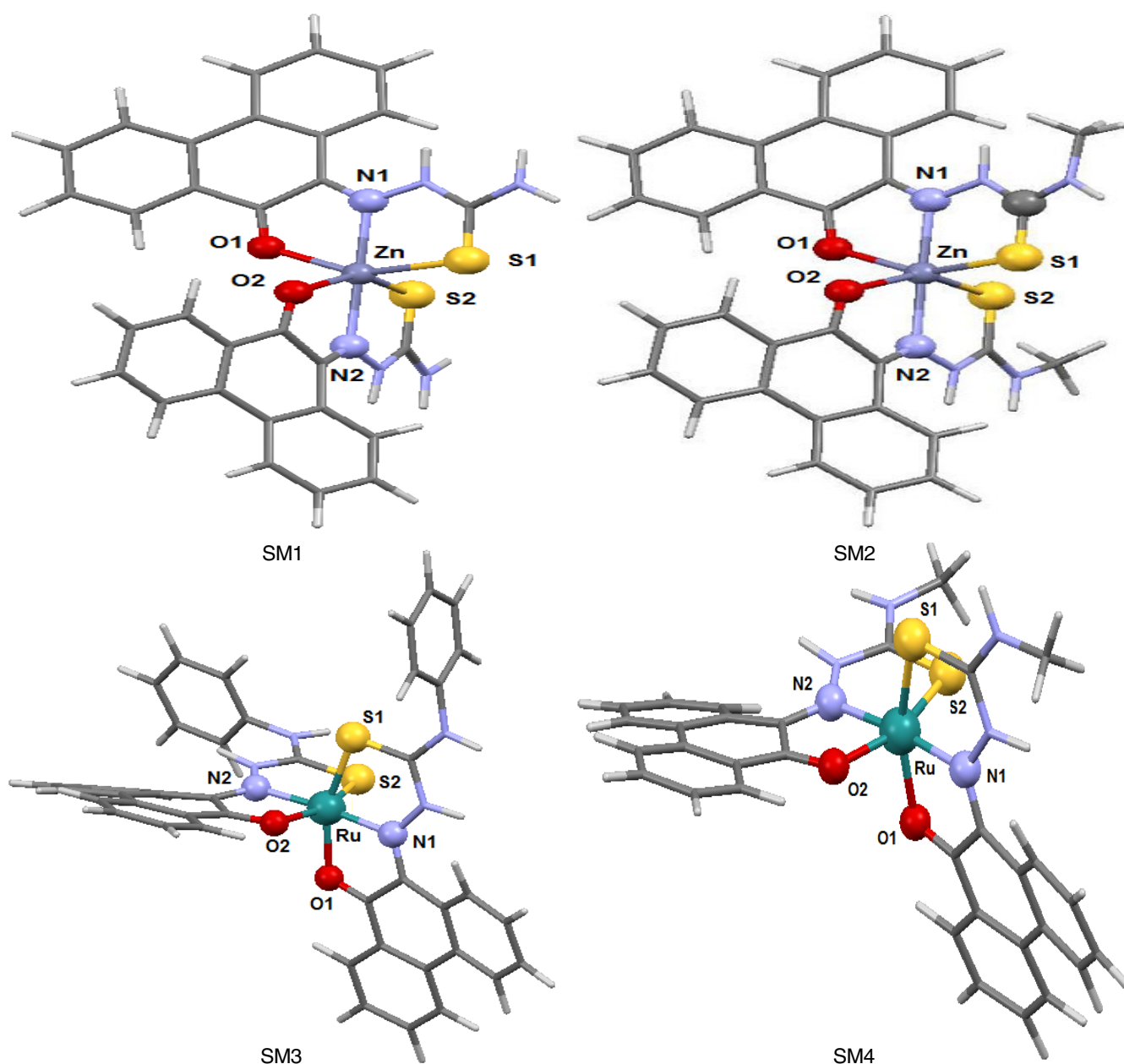


Fig. 1. Perspective view of the optimized geometry of the metal complexes

TABLE-1
OPTIMIZED GEOMETRICAL PARAMETER FOR THE METAL COMPLEXES BOND LENGTH (Å) AND BOND ANGLE (°)

Bond length (Å)	SM1	SM2	Bond length (Å)	SM3	SM4
Ru-O1	2.147	2.152	Zn-O1	2.124	2.131
Ru-O2	2.148	2.147	Zn-O2	2.136	2.129
Ru-S1	2.548	2.532	Zn-S1	2.415	2.415
Ru-S2	2.545	2.543	Zn-S2	2.414	2.413
Ru-N1	2.286	2.293	Zn-N1	2.032	2.030
Ru-N2	2.287	2.287	Zn-N2	2.027	2.030
Bond angle (°)	SM1	SM2	Bond angle (°)	SM3	SM4
O1-Ru-N1	76.14	76.11	O1-Ru-N1	76.14	76.11
O1-Ru-S1	159.75	159.65	O1-Ru-S1	159.75	159.65
N1-Ru-S1	83.70	83.67	N1-Ru-S1	83.70	83.67
O1-Ru-S2	90.10	89.92	O1-Ru-S2	90.10	89.92
O1-Ru-N2	99.54	99.50	O1-Ru-N2	99.54	99.50
O1-Ru-O2	95.26	95.31	O1-Ru-O2	95.26	95.31
O2-Ru-S2	159.73	159.70	O2-Ru-S2	159.73	159.70
O2-Ru-N2	76.06	76.12	O2-Ru-N2	76.06	76.12
S2-Ru-N2	83.78	83.68	S2-Ru-N2	83.78	83.68

Biological activity

Antimycobacterial screening: The initial antimycobacterial susceptibility testing at 100 μM of compounds using resazurin microtiter plate assay resulted in growth inhibition. The metal-complexes *viz.* the SM2, SM3 and SM4, showed good inhibition at 100 μM concentration (Fig. 2). The MIC determination studies indicate that SM2, SM3 and SM4 showed maximum inhibition at 100 μM and subsequently concentration dependent growth inhibition was observed lower inhibition being observed as the concentration was reduced (Fig. 3). In case of SM2, the inhibition observed was around 80% from higher to lower concentration (6.25 μM), suggesting its inhibition was not much affected by concentration of compound studied, as the lower concentration of compound was as effective as higher concentration. This could be due to the compound being bacteriostatic in nature and the fluorescence being observed was due to the fluorescence of cells coming from inoculum, which although were not able to grow further during incubation period, were showing the observed fluorescence. Complex SM2 even at the lower concentration shows good growth inhibition and will be studied further to improve its antimycobacterial activity improvement. The drug susceptibility studies (DST) using 96-well plate assays using fluore-

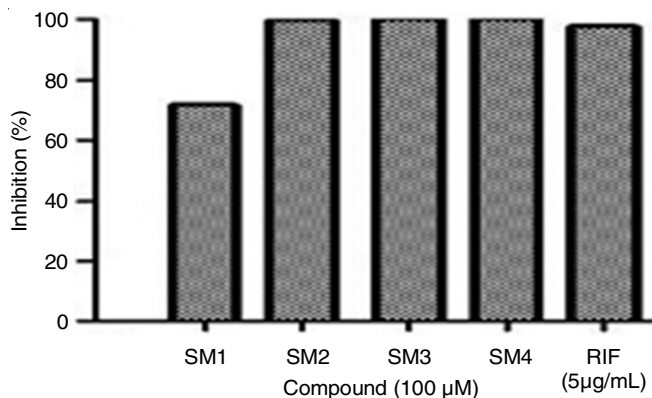


Fig. 2. Initial screening at 100 μM concentration of compounds. Rifampicin (RIF) was used as inhibition control

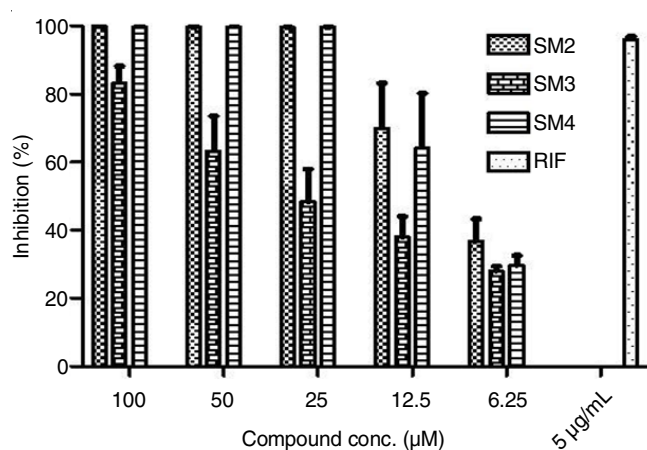


Fig. 3. MIC studies for selected compounds starting with the initial concentration of 100 μM . Rifampicin (RIF) were used as inhibition control

scence or colorimetric methods are low cost alternatives to MGIT and BACTEC systems with good correlation [26]. The colorimetric indicators such as Alamar blue, MTT and resazurin have been found to have good specificity and hence resazurin was used in this study. Cytotoxic studies in THP-1 cells show complexes SM3 and SM4 were cytotoxic at 10X, 5X and 2.5X MIC (Fig. 4).

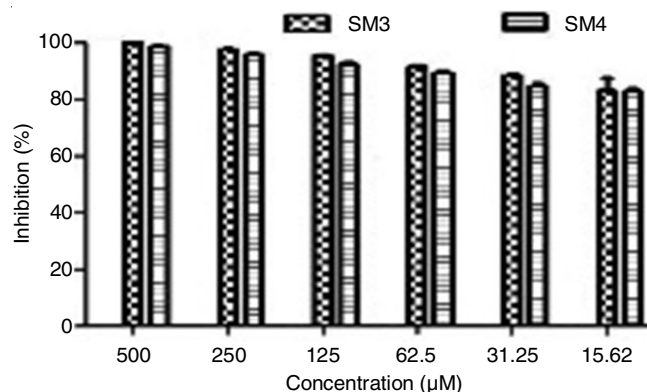


Fig. 4. Cytotoxicity studies in THP-1 cells. The compounds SM3 and SM4 were cytotoxic at 10X, 5X and 2.5X MIC

The DNA mobility shift studies show Lane 1 is untreated DNA control. Lane 2 is DNA incubated with compound SM2, lane 3 is DNA incubated with SM3, lane 4 is 1kb DNA ladder (MBI Fermentas), no shift in mobility was observed after 4 h incubation at 100 μ M concentrations of compounds (Fig. 5).

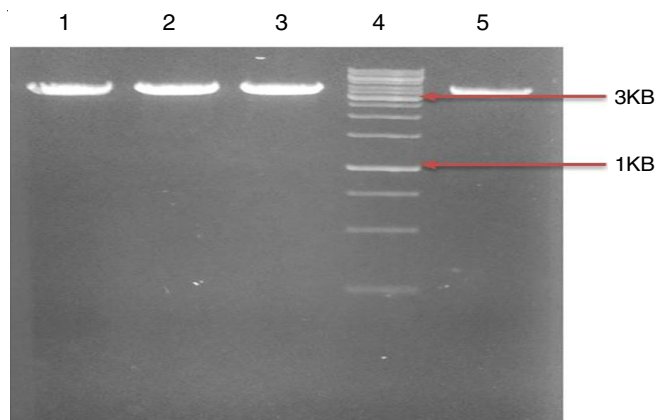


Fig. 5. DNA mobility shift studies. Lane 1 is untreated DNA control. Lane 2 is DNA incubated with compound SM2, lane 3 is DNA incubated with SM3, lane 4 is 1 kb DNA ladder (MBI Fermentas), No shift in mobility was observed after 4 h incubation at 100 μ M concentrations of compounds

Conclusion

Three tridentate phenanthroquinone ligands (HL1-HL3) and their zinc(II) and ruthenium(II) complexes (SM1-SM4) were synthesized and characterized by spectroscopic methods and other physical measurements. The geometry of the synthesized complexes was optimized using Gaussian-09. These data found good agreement with proposed octahedral structure of metal complexes. Zinc(II) and ruthenium(II) complexes were screened for the antimycobacterial activity at 100 μ M of compounds using resazurin microtiter plate assay resulted in growth inhibition. The complexes SM2, SM3 and SM4, showed good antimycobacterial activity at 100 μ M concentrations.

ACKNOWLEDGEMENTS

The authors are thankful to The Head, Department of Chemistry, University of Lucknow, Lucknow, India and Central Facility for Computational Research for providing the research facilities. The authors are also thankful to The Director, SAIF, CDRI, Lucknow, India, for providing the spectral analysis and support for carrying the biological studies. The financial support from CSIR, New Delhi, India for providing the JRF to one of the authors (SKS) (File No. 09/107(0383)/2017) is also gratefully acknowledged.

CONFLICT OF INTEREST

The authors declare that there is no conflict of interests regarding the publication of this article.

REFERENCES

1. A. Thakur, H. Mikkelsen and G. Jungersen, *J. Immunol. Res.*, **2019**, 1356540 (2019); <https://doi.org/10.1155/2019/1356540>
2. S.G. Kurz, J.J. Furin and C.M. Bark, *Infect. Dis. Clin. North Am.*, **30**, 509 (2016); <https://doi.org/10.1016/j.idc.2016.02.010>
3. M.T. Heinrichs, R.J. May, F. Heider, T. Reimers, S.K.B. Sy, C.A. Peloquin and H. Derendorf, *Int. J. Mycobacteriol.*, **7**, 156 (2018); https://doi.org/10.4103/ijmy.ijmy_33_18
4. J. van den Boogaard, G.S. Kibiki, E.R. Kisanga, M.J. Boeree and R.E. Aarnoutse, *Antimicrob. Agents Chemother.*, **53**, 849 (2009); <https://doi.org/10.1128/AAC.00749-08>
5. T. Törün, G. Güngör, I. Ozmen, Y. Bölükbaşı, E. Maden, B. Bıçakçı, G. Ataç, T. Sevim and K. Tahaoglu, *Int. J. Tuberc. Lung Dis.*, **9**, 1373 (2005).
6. L.Z. Montelongo-Peralta, A. León-Buitimea, J.P. Palma-Nicolás, J. Gonzalez-Christen and J.R. Morones-Ramírez, *Sci. Rep.*, **9**, 5471 (2019); <https://doi.org/10.1038/s41598-019-42049-5>
7. Y. Yoshikawa and H. Yasui, *Curr. Top. Med. Chem.*, **12**, 210 (2012); <https://doi.org/10.2174/156802612799078874>
8. C. Mari, V. Pierroz, S. Ferrari and G. Gasser, *Chem. Sci.*, **6**, 2660 (2015); <https://doi.org/10.1039/C4SC03759F>
9. J.L. Bolton and T. Dunlap, *Chem. Res. Toxicol.*, **30**, 13 (2017); <https://doi.org/10.1021/acs.chemrestox.6b00256>
10. N. El-Najjar, H. Gali-Muhtasib, R.A. Ketola, P. Vuorela, A. Urtti and H. Vuorela, *Phytochem. Rev.*, **10**, 353 (2011) <https://doi.org/10.1007/s11101-011-9209-1>
11. Z. Afrasiabi, E. Sinn, S. Padhye, S. Dutta, S. Padhye, C. Newton, C.E. Anson and A.K. Powell, *J. Inorg. Biochem.*, **95**, 306 (2003); [https://doi.org/10.1016/S0162-0134\(03\)00131-4](https://doi.org/10.1016/S0162-0134(03)00131-4)
12. P. Anitha, P. Viswanathamurthi, D. Kesavan and R.J. Butcher, *J. Coord. Chem.*, **68**, 321 (2015); <https://doi.org/10.1080/00958972.2014.977269>
13. S. Padhye, Z. Afrasiabi, E. Sinn, J. Fok, K. Mehta and N. Rath, *Inorg. Chem.*, **44**, 1154 (2005); <https://doi.org/10.1021/ic048214v>
14. P. Anitha, N. Chitrapriya, Y.J. Jang and P. Viswanathamurthi, *J. Photochem. Photobiol. B: Biol.*, **129**, 17 (2013); <https://doi.org/10.1016/j.jphotobiol.2013.09.005>
15. A.E. Stacy, D. Palanimuthu, P.V. Bernhardt, D.S. Kalinowski, P.J. Jansson and D.R. Richardson, *J. Med. Chem.*, **59**, 4965 (2016); <https://doi.org/10.1021/acs.jmedchem.6b00238>
16. S.S. Karki, S. Thota, S.Y. Darj, J. Balzarini and E. De Clercq, *Bioorg. Med. Chem.*, **15**, 6632 (2007); <https://doi.org/10.1016/j.bmc.2007.08.014>
17. J.-C. Palomino, A. Martin, M. Camacho, H. Guerra, J. Swings and F. Portaels, *Antimicrob. Agents Chemother.*, **46**, 2720 (2002); <https://doi.org/10.1128/AAC.46.8.2720-2722.2002>
18. X. Liao, J. Lu, P. Ying, P. Zhao, Y. Bai, W. Li and M. Liu, *J. Biol. Inorg. Chem.*, **18**, 975 (2013); <https://doi.org/10.1007/s00775-013-1046-9>
19. B.J. Hathaway and D.E. Billing, *Coord. Chem. Rev.*, **5**, 143 (1970); [https://doi.org/10.1016/S0010-8545\(00\)80135-6](https://doi.org/10.1016/S0010-8545(00)80135-6)
20. A.K. Singh, G. Saxena, L. Kumari, S.K. Singh, M. Faheem, A. Kumar and R. Sharma, *Lett. Appl. NanoBioSci.*, **10**, 1760 (2021); <https://doi.org/10.33263/LIANBS101.17601791>
21. C. He, S. Yu, S. Ma and F. Cheng, *Transition Met. Chem.*, **44**, 515 (2019); <https://doi.org/10.1007/s11243-019-00309-3>
22. P. Miotto, Y. Zhang, D.M. Cirillo and W.C. Yam, *Respirology*, **23**, 1098 (2018); <https://doi.org/10.1111/resp.13393>
23. S. Xu, J.E.T. Smith and J.M. Weber, *J. Chem. Phys.*, **145**, 024304 (2016); <https://doi.org/10.1063/1.4955262>
24. T.R. Arun and N. Raman, *Spectrochim. Acta A Mol. Biomol. Spectrosc.*, **127**, 292 (2014); <https://doi.org/10.1016/j.saa.2014.02.074>
25. O.G. Idemudia and E.C. Hosten, *Crystals*, **6**, 127 (2016); <https://doi.org/10.3390/cryst6100127>
26. E. Montoro, D. Lemus, M. Echemendia, *J. Antimicrob. Chemother.*, **55**, 500 (2005); <https://doi.org/10.1093/jac/dki023>